

Mesoscopic wave turbulence.

V. E. Zakharov^{+,*†}, A. O. Korotkevich⁺¹⁾, A. N. Pushkarev^{+‡}, A. I. Dyachenko⁺

⁺*L.D. Landau Institute for Theoretical Physics RAS, 2 Kosygin Str., Moscow, 119334 Russian Federation*

^{*}*Department of Mathematics, University of Arizona, Tucson, AZ 85721 USA*

[‡]*Waves and Solitons LLC, 738 W. Sereno Dr., Gilbert, AZ 85233 USA*

Submitted 16 August 2005

We report results of simulation of wave turbulence. Both inverse and direct cascades are observed. The definition of "mesoscopic turbulence" is given. This is a regime when the number of modes in a system involved in turbulence is high enough to qualitatively simulate most of the processes but significantly smaller than the threshold, which gives us quantitative agreement with the statistical description, such as kinetic equation. Such a regime takes place in numerical simulation, in essentially finite systems, etc.

PACS: 02.60Cb, 47.11.+j, 47.35.+i, 47.27.Eq

The theory of wave turbulence is developed for infinitely large system. In weakly nonlinear dispersive media, the turbulence is described by a kinetic equation for squared wave amplitudes (weak turbulence). However, all real systems are finite. Computer simulation of wave turbulence can also be performed only in finite system (typically in a box with periodic boundary conditions). It is important to know how strong discreteness of a system impacts the physical picture of wave turbulence.

Let a turbulence be realized in a Q -dimensional cube with side L . Then, wave vectors form a cubic lattice with the lattice constant $\Delta k = 2\pi/L$. Suppose that four-wave resonant conditions are dominating. Exact resonances satisfy the equations

$$\mathbf{k} + \mathbf{k}_1 - \mathbf{k}_2 - \mathbf{k}_3 = 0, \quad (1)$$

$$\Delta = \omega(k) + \omega(k_1) - \omega(k_2) - \omega(k_3) = 0. \quad (2)$$

In infinite medium, Eqs. (1) and (2) define hypersurface of dimension $3Q - 1$ in $4Q$ -dimensional space $\mathbf{k}, \mathbf{k}_1, \mathbf{k}_2, \mathbf{k}_3$. In a finite system, (1) and (2) are Diophantine equations which might have or have no exact solutions. The Diophantine equation for four-wave resonant processes are not studied yet. For three-wave resonant processes, they are studied for Rossby waves on the β -plane [1].

However, not only exact resonances are important. Individual harmonics in the wave ensemble fluctuate with inverse time $\Gamma_{\mathbf{k}}$, dependent on their wavenumbers. Suppose that all $\Gamma_{\mathbf{k}_i}$ for waves, composing a resonant quartet, are of the same order of magnitude $\Gamma_{\mathbf{k}_i} \sim \Gamma$. Then resonant equation (2) has to be satisfied up to

¹⁾e-mail: kao@landau.ac.ru

accuracy $\Delta \sim \Gamma$, and the resonant surface is blurred into the layer of thickness $\delta k/k \simeq \Gamma_k/\omega_k$. This thickness should be compared with the lattice constant Δk . Three different cases are possible

1. $\delta k \gg \Delta k$. In this case the resonant layer is thick enough to hold many approximate resonant quartets on a unit of resonant surface square. These resonances are dense, and the theory is close to the classical weak turbulent theory in infinite media. The weak turbulent theory offers recipes for calculation of Γ_k . The weak-turbulent Γ_k are the smallest among all given by theoretical models. To be sure that the case is realized, one has to use weak-turbulent formulae for Γ_k .
2. $\delta k < \Delta k$. This is the opposite case. Resonances are rarefied, and the system consists of a discrete set of weakly interacting oscillators. A typical regime in this situation is the "frozen turbulence" [2], [3], [4], which is actually a system of KAM tori, accomplished with a weak Arnold's diffusion.
3. The intermediate case $\delta k \simeq \Delta k$ can be called "mesoscopic turbulence". The density of approximate resonances is high enough to provide the energy transport along the spectrum, but low enough to guarantee "equal rights" for all harmonics, which is a necessary condition for applicability of the weak turbulent theory.

In this article we report results of our numerical experiments on modeling of turbulence of gravity waves on the surface of deep ideal incompressible fluid. The motivation for this work was numerical justification of

Hasselmann kinetic equation. The result is discovery of the mesoscopic turbulence. The fluid motion is potential and described by shape of surface $\eta(\mathbf{r}, t)$ and velocity potential $\psi(\mathbf{r}, t)$, evaluated on the surface. These variables satisfy the canonical equations [5]

$$\frac{\partial \eta}{\partial t} = \frac{\delta H}{\delta \psi}, \quad \frac{\partial \psi}{\partial t} = -\frac{\delta H}{\delta \eta}, \quad (3)$$

Hamiltonian H is presented by the first three terms in expansion on powers of nonlinearity $\nabla \eta$

$$\begin{aligned} H &= H_0 + H_1 + H_2 + \dots, \\ H_0 &= \frac{1}{2} \int (g\eta^2 + \psi \hat{k} \psi) \, dx dy, \\ H_1 &= \frac{1}{2} \int \eta [|\nabla \psi|^2 - (\hat{k} \psi)^2] \, dx dy, \\ H_2 &= \frac{1}{2} \int \eta (\hat{k} \psi) [\hat{k} (\eta (\hat{k} \psi)) + \eta \nabla^2 \psi] \, dx dy. \end{aligned} \quad (4)$$

Thereafter, we put gravity acceleration equal to $g = 1$. Here, \hat{k} is a linear integral operator ($\hat{k} = \sqrt{-\nabla^2}$), such that, in k -space, it corresponds to multiplication of Fourier harmonics ($\psi_{\mathbf{k}} = \frac{1}{2\pi} \int \psi_{\mathbf{r}} e^{i\mathbf{k}\mathbf{r}} \, dx dy$) by $\sqrt{k_x^2 + k_y^2}$. For gravity waves, this reduced Hamiltonian describes four-wave interaction. Then, dynamical equations (3) acquire the form

$$\begin{aligned} \dot{\eta} &= \hat{k} \psi - (\nabla(\eta \nabla \psi)) - \hat{k}[\eta \hat{k} \psi] + \\ &\quad + \hat{k}(\eta \hat{k}[\eta \hat{k} \psi]) + \frac{1}{2} \nabla^2[\eta^2 \hat{k} \psi] + \frac{1}{2} \hat{k}[\eta^2 \nabla^2 \psi], \\ \dot{\psi} &= -g\eta - \frac{1}{2} [(\nabla \psi)^2 - (\hat{k} \psi)^2] - \\ &\quad - [\hat{k} \psi] \hat{k}[\eta \hat{k} \psi] - [\eta \hat{k} \psi] \nabla^2 \psi. \end{aligned} \quad (5)$$

Let us introduce the canonical variables $a_{\mathbf{k}}$ as shown below

$$a_{\mathbf{k}} = \sqrt{\frac{\omega_{\mathbf{k}}}{2k}} \eta_{\mathbf{k}} + i \sqrt{\frac{k}{2\omega_{\mathbf{k}}}} \psi_{\mathbf{k}}, \quad (6)$$

where $\omega_{\mathbf{k}} = \sqrt{gk}$. In these so called normal variables equations (3) take the form

$$\frac{\partial a_{\mathbf{k}}}{\partial t} = -i \frac{\delta H}{\delta a_{\mathbf{k}}^*}. \quad (7)$$

The physical meaning of these variables is quite clear: $|a_{\mathbf{k}}|^2$ is an action spectral density, or $|a_{\mathbf{k}}|^2 \Delta k^2$ is a number of particles with the particular wave number \mathbf{k} .

We solved equations (5) numerically in a box $2\pi \times 2\pi$ using a spectral code on rectangular grid with double periodic boundary conditions. The implicit energy-preserving scheme, similar to used in [6], [7], [8], was implemented. We studied evolution of freely propagating waves (swell) in the absence of wind in the spirit of paper [9]. Different grids (512×512 , 256×1024 ,

256×2048) with different initial data were tried. In all the cases, we observed mesoscopic wave turbulence. The most spectacular results are achieved on the grid 256×2048 .

As initial conditions, we used a Gauss-shaped distribution on a long axis of the wavenumbers plane

$$\begin{cases} |a_{\mathbf{k}}| = A_i \exp\left(-\frac{1}{2} \frac{|\mathbf{k} - \mathbf{k}_0|^2}{D_i^2}\right), & |\mathbf{k} - \mathbf{k}_0| \leq 2D_i, \\ |a_{\mathbf{k}}| = 10^{-12}, & |\mathbf{k} - \mathbf{k}_0| > 2D_i, \end{cases} \quad (8)$$

$A_i = 5 \times 10^{-6}, D_i = 30, \mathbf{k}_0 = (0; 150).$

The initial phases of all the harmonics were random. The average steepness $\mu = \langle |\nabla \eta| \rangle \simeq 0.115$. To stabilize the computations in the high-frequency region [10], we introduced artificial damping, mimicking viscosity at small scales, and an artificial smoothing term to the equation for the surface evolution

$$\begin{aligned} \frac{\partial \psi_{\mathbf{k}}}{\partial t} &\rightarrow \frac{\partial \psi_{\mathbf{k}}}{\partial t} + \gamma_k \psi_{\mathbf{k}}, \\ \frac{\partial \eta_{\mathbf{k}}}{\partial t} &\rightarrow \frac{\partial \eta_{\mathbf{k}}}{\partial t} + \gamma_k \eta_{\mathbf{k}}, \\ \gamma_k &= \begin{cases} 0, & k < k_d, \\ -\gamma(k - k_d)^2, & k \geq k_d, \end{cases} \\ k_d &= 512, \gamma = 2 \times 10^4, \tau = 3.1 \times 10^{-4}. \end{aligned} \quad (9)$$

With the time step τ , this calculations took about two months on AMD Athlon 64 3500+ computer. During this time, we reached 1500 periods of the wave in the initial spectral maximum.

The process of waves evolution can be separated in two steps. On the first stage (about fifty initial wave periods), we observe fast loss of energy and wave action. This effect can be explained by formation of "slave" harmonics taking their part of motion constants. Initially smooth spectrum becomes very rough. The spectral maximum demonstrates fast downshift.

In the second stage, the downshift continues but all processes slow down. Plots of energy, wave action, mean frequency, and mean steepness are presented in Figs. 1-4. One can see clear tendency to downshift of the spectral maximum corresponding to inverse cascade; however, this process is more slow than predicted by the weak turbulence theory. Self-similar downshift in this theory gives [11], [12]

$$\omega \sim t^{-1/11}.$$

In our experiments

$$\omega \sim t^{-\alpha},$$

where α decreases with time from 1/16 to 1/20. Evolution of angle averaged spectra $N_k = \int_0^{2\pi} |a_{\mathbf{k}}|^2 k d\mathbf{k} d\vartheta$ is

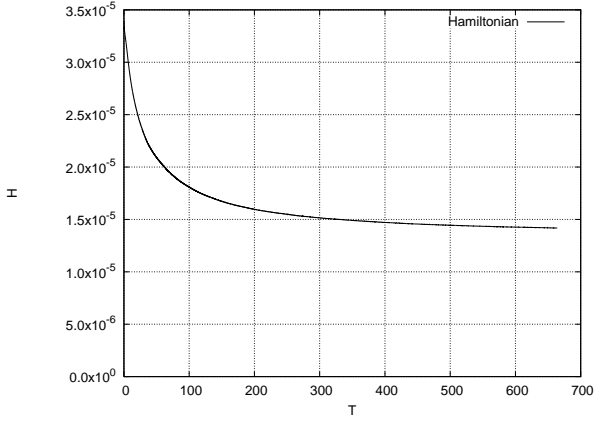


Fig.1. Total energy of the system.

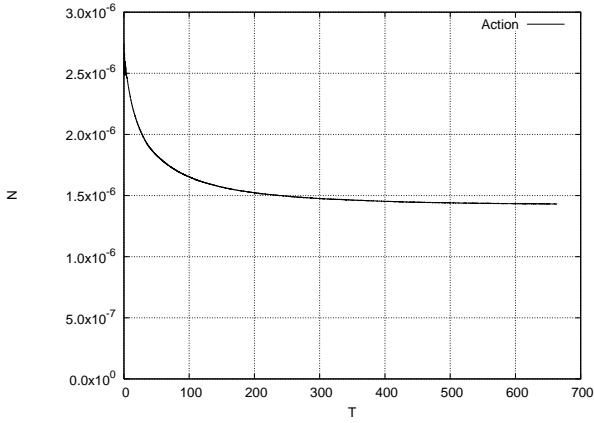


Fig.2. Total action of the system.

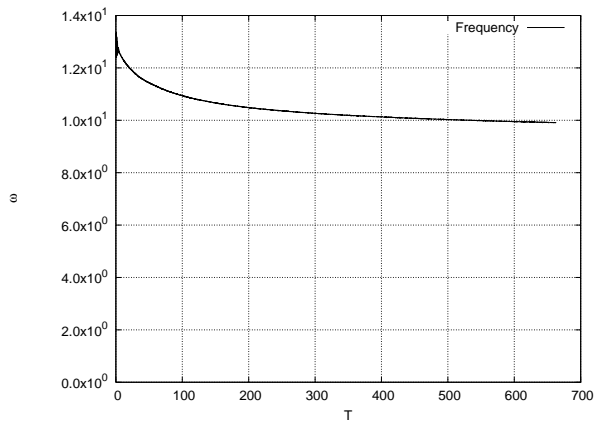


Fig.3. Frequency of the spectral maximum.

presented on Fig. 5. Their tails (Fig. 6) are Zakharov-Filonenko weak-turbulent Kolmogorov spectra [13] corresponding to direct cascade

$$|a_k|^2 \sim \frac{1}{k^4}. \quad (10)$$

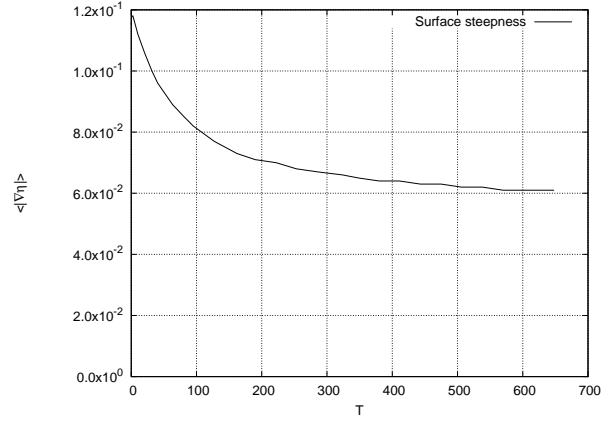


Fig.4. Mean steepness of fluid surface.

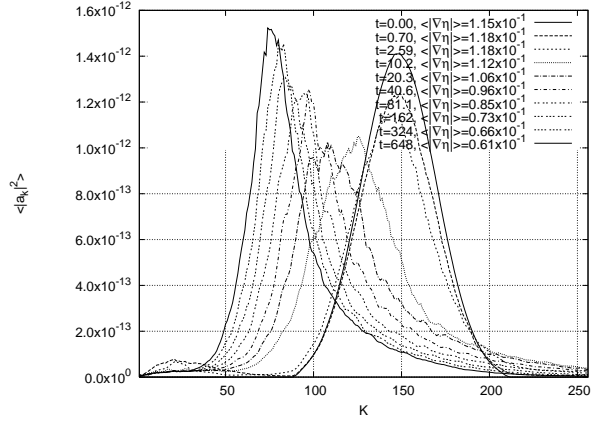
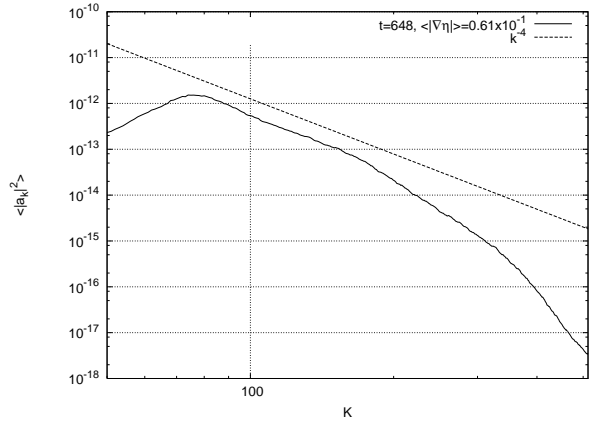


Fig.5. Averaged with angle spectra. Downshift of spectral maximum is clearly observable.

This result is robust; it was observed in similar calculations [9], [7], [8].


 Fig.6. Tails of angle-averaged spectrum in double logarithmic scale. $T = 648 = 1263T_0$. Power-like tail and front slope are close to predicted by the weak turbulent theory.

Two dimensional spectra in the initial and in the last moments of calculations are presented in Fig. 7, 8. One can see formation of small intensity "jets" posed on the Phillips resonant curve [14]

$$2\omega(\mathbf{k}_0) = \omega(\mathbf{k}_0 + \mathbf{k}) + \omega(\mathbf{k}_0 - \mathbf{k}). \quad (11)$$

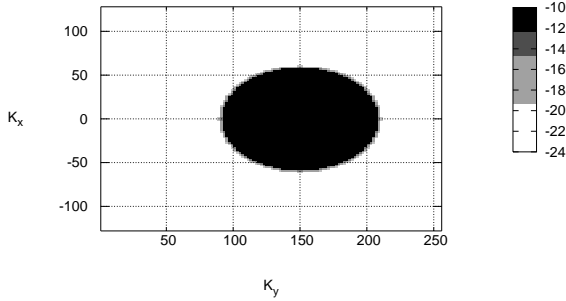


Fig.7. Level lines of logarithm of initial spectra distribution. $T = 0$.

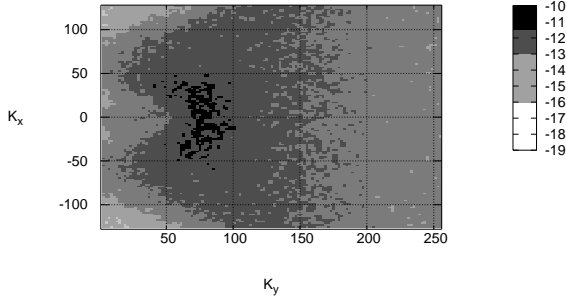


Fig.8. Level lines of logarithm of spectra distribution at $T = 648 = 1263T_0$.

The spectra are very rough and sharp. The slice of spectra along the line $(0; k_y)$ in the end of the computations is presented on Fig. 9. Evolution of squared wave amplitudes for a cluster of neighbouring harmonics is presented in Fig. 10.

Results presented in Fig. 10 show that what we modeled is mesoscopic turbulence. Indeed, characteristic time of amplitude evolution on a figure is a hundred or more their periods; thus Γ/ω_k is comparable

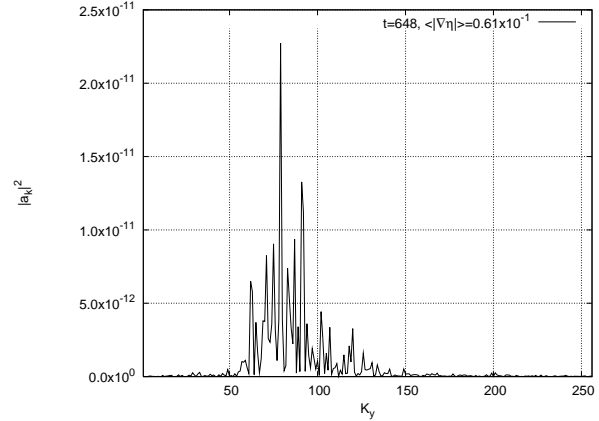


Fig.9. Slice of spectrum on axis $(0; k_y)$ at $T = 648 = 1263T_0$.

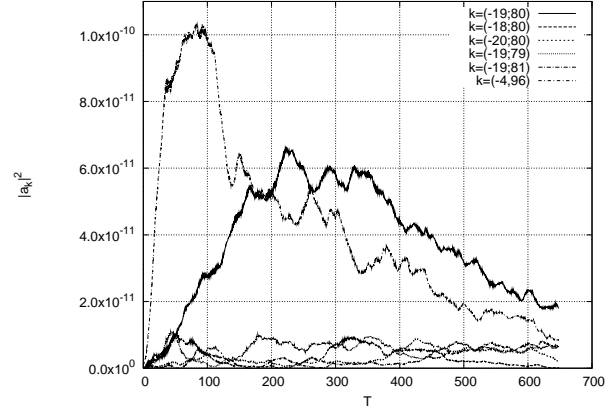


Fig.10. Evolution of some cluster of harmonics and a distant large harmonic.

with $\Delta k/k$. On the same figure we can see the most remarkable features of such turbulence.

The weak turbulence in the first approximation obeys the Gaussian statistics. The neighbouring harmonics are uncorrelated and statistically independent ($\langle a_k a_{k+1}^* \rangle = 0$). However, their averaged characteristics are close to each other. This is a "democratic society". On the contrary mesoscopic turbulence is an "oligarchic society". The Phillips curve (11) has a genus 2. After Faltings' proof [15] of Mordell's hypothesis [16] we know that the number of solutions of the Diophantine equation

$$\Delta = 2(n^2 + m^2)^{1/4} - [(n+x)^2 + (m+y)^2]^{1/4} - [(n-x)^2 + (m-y)^2]^{1/4} = 0 \quad (12)$$

is at most finite and most probably, except for a few trivial solutions, equals to zero. The same statement

is very plausible for more general resonances. Approximate integer solutions in the case

$$|\Delta| < \epsilon$$

do exist, but their number fast tends to zero at $\epsilon \rightarrow 0$. Classification of these solutions is a hard problem of the number theory. These solutions compose the "elite society" of the harmonics, which play the most active role in the mesoscopic turbulence. Almost all the inverse cascade of wave action is realized within members of this "privileged club". The distribution of the harmonics exceeding the reference level $|a_k|^2 = 10^{-11}$ at the moment $t = 1200T_0$ is presented in Fig. 11. The number of such harmonics is not more than 600, while the total number of harmonics involved into the turbulence is of the order of 10^4 .

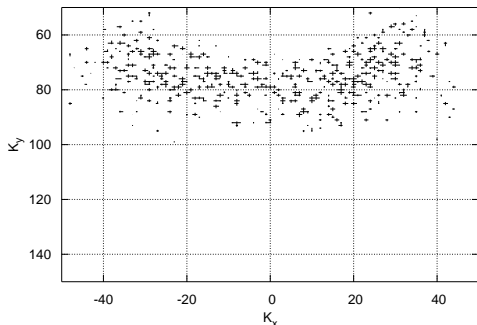


Fig.11. Harmonics with square modulus exceeding the level 10^{-11} at $T = 648 = 1263T_0$.

Note that a situation with direct cascade is different. As far as the coupling coefficient for gravity waves growth as fast as k^3 with the wave number, for short waves Γ_k/ω_k easily exceeds $\Delta k/k$, and the conditions of applicability of the weak turbulent theory for short waves are satisfied.

Note also that the mesoscopic turbulence is not a numerical artefact. Simple estimations show that, for gravity waves, it is realized in some conditions in basins of a moderate size, like small lakes as well as in experimental wave tanks. It is also common for long internal waves in the ocean and for inertial gravity waves in atmosphere, for plasma waves in tokamaks, etc.

This work was supported by RFBR grant 03-01-00289, the Programme "Nonlinear dynamics and solitons" of the RAS Presidium and "Leading Scientific Schools of Russia" grant, also by ONR grant N00014-03-1-0648, US Army Corps of Engineers, RDT&E Programm W912HZ-04-P-0172, Grant DACA 42-00-C0044.

We use this opportunity to gratefully acknowledge the support of these foundations.

Also, the authors want to thank creators of the open-source fast Fourier transform library FFTW [17] for this fast, portable and completely free piece of software.

1. G. Reznik, L. Piterbarg, E. Kartashova, *Dyn. Atm. Oceans*, **18**, 235 (1993).
2. A. N. Pushkarev and V. E. Zakharov, *Physica D*, **155**, 98 (1999).
3. A. N. Pushkarev, *Eur. J. of Mech. B/Fluids*, **18**, 3, 345 (1999).
4. C. Connaughton, S. Nazarenko and A. Pushkarev, *Phys. Rev. E*, **63**, 046306 (2001).
5. V. E. Zakharov, *J. Appl. Mech. Tech. Phys.* **2**, 190 (1968).
6. A. I. Dyachenko, A. O. Korotkevich and V. E. Zakharov, *Pis'ma v ZhETF* **77**, 9, 572 (2003); (english transl. *JETP Lett.* **77**, 9, 477 (2003)). arXiv:physics/0308100
7. A. I. Dyachenko, A. O. Korotkevich and V. E. Zakharov, *Pis'ma v ZhETF* **77**, 10, 649 (2003); (english transl. *JETP Lett.* **77**, 10, 546 (2003)). arXiv:physics/0308101
8. A. I. Dyachenko, A. O. Korotkevich and V. E. Zakharov, *Phys. Rev. Lett.* **92**, 13, 134501 (2004). arXiv:physics/0308099
9. M. Onorato, A. R. Osborne, M. Serio et al., *Phys. Rev. Lett.* **89**, 14, 144501 (2002). arXiv:nlin.CD/0201017
10. P. M. Lushnikov and V. E. Zakharov, **203**, 9 (2005). arXiv:nlin.PS/0410054
11. V. E. Zakharov, Ph.D. thesis, G.I. Budker Institute for Nuclear Physics, Novosibirsk, USSR (1966).
12. V. E. Zakharov and M. M. Zaslavskii, *Izv. Atm.Ocean.Phys.* **18**, 747 (1982).
13. V. E. Zakharov and N. N. Filonenko, *J. Appl. Mech. Tech. Phys.* **4**, 506 (1967).
14. Phillips, O.M., *J. Fluid Mech.* **107**, 465-485, (1981).
15. G. Faltings, *Invent. Math.* **73**, 3, 349 (1983); Erratum: *Invent. Math.* **75**, 2, 381 (1984).
16. L. J. Mordell, *Proc. Cambridge Phil. Soc.* **21**, 179 (1922).
17. <http://fftw.org>